

# Catalytic effect of commercial nano-CuO and nano-Fe<sub>2</sub>O<sub>3</sub> on thermal decomposition of ammonium perchlorate

Mostafa Mahinroosta<sup>1\*</sup>

\* Corresponding author

Email: mahinroosta2010@gmail.com

<sup>1</sup> No. 8, Negarestan 4, Nazarabad, Alborz 3331779638, Iran

## Abstract

Size reduction of the catalyst increases the surface area, and hence, the catalytic activity is also increased. The decrease in temperature of decomposition of ammonium perchlorate in the presence of nano-copper oxide and nano-ferric oxide is investigated within the scope of this study. Different mixes of ammonium perchlorate with nano-ferric oxide and nano-copper oxide were prepared. Differential scanning calorimetry test results show that addition of nanometer-sized ferric oxide and copper oxide leads to a significant decrease in higher decomposition temperature of ammonium perchlorate. The most significant decrease in the decomposition temperature was observed in the presence of 3% of nano-copper oxide.

## Keywords

Ammonium perchlorate, Thermal decomposition, Catalyst, Nanostructure

## Background

At nanoscale, the physicochemical characteristics of materials are considerably various from those found in larger scales and bulk materials [1]. Nanoparticles have many noteworthy properties due to their small size and very large specific surface area [2]. There is a growing interest in the synthesis and use of metal or metal oxide nanoparticles due to their large specific surface area and high activity in most catalytic processes [3,4]. It is noted that nanoparticles are not only effective in the catalytic processes such as gas-solid, gas-liquid-solid or liquid-solid, where the nanoparticles, as the catalyst, are the solid phase, but also effective in the solid-solid catalytic processes [5]. Transition metal oxide nanoparticles exhibit a broad class of materials that have been investigated extensively due to their interesting catalytic properties and wide scope of their potential applications [6]. It has been proven that nanometer-sized metals and metal oxides are effective to improve the decomposition of ammonium perchlorate (AP) [3-5,7-14]. Although the characteristics of AP thermal decomposition can be tailored to some extent by decreasing the particle size of AP, this method is rarely used due to the dangerousness of superfine AP [5,15]. Particle size distribution, morphology, and nanostructure of particles are very important characteristics and affect the kinetics of decomposition of AP [4]. Many researchers have studied the catalytic effects of nanostructures such as nanometer-sized metals and metal oxides on the thermal decomposition of AP and observed their tailoring effect on the thermal decomposition behavior of AP [3-5,7-14]. Table 1 presents a historical background about

some important events in the field of the effect of nanostructures on thermal decomposition of AP. In this paper, the catalytic effect of commercial nano-sized ferric oxide and nano-sized copper oxide on the thermal decomposition of AP is investigated.

**Table 1 Bibliographic history of the effect of nanostructure on thermal decomposition of AP**

Author	Year	Significance
Weifan et al. [7]	2006	Nano-sized yttria
Meda et al. [8]	2007	Nano-aluminum
Duan et al. [16]	2007	Nano-sized MgO
Liu et al. [15]	2008	Nanometer-sized $\text{CuFe}_2\text{O}_4$
Duan et al. [5]	2008	Ni nanoparticles
Hongzhen et al. [3]	2008	Co nanoparticles
Satyawati et al. [4]	2008	Nano-ferric oxide
Wang et al. [9]	2009	CuO nanocrystals
Aijun et al. [10]	2011	Nano- $\text{MnFe}_2\text{O}_4$
Zhang et al. [11]	2011	Nano $\alpha\text{-Fe}_2\text{O}_3$
Zhou et al. [12]	2011	$\text{ZnO/AP}$ , $\text{Co}_3\text{O}_4/\text{AP}$ , $\text{Fe}_2\text{O}_3/\text{AP}$ nanocomposites
Chaturvedi and Dave [13]	2011	Nanometals
Alizadeh et al. [14]	2012	Nano-sized CuO, $\text{Co}_3\text{O}_4$ , and $\text{CuCo}_2\text{O}_4$

## Results and discussion

Transmission emission microscopy (TEM) images of nano-CuO and nano- $\text{Fe}_2\text{O}_3$  are shown in Figure 1. From this figure, it can be observed that the morphology of these nanoparticles is relatively spherical. Figure 2 shows the X-ray diffraction (XRD) patterns of commercial nano-CuO and nano- $\text{Fe}_2\text{O}_3$ .

**Figure 1 TEM images of (a) nano-CuO and (b) nano- $\text{Fe}_2\text{O}_3$ .**

**Figure 2 XRD patterns of (a) nano- $\text{Fe}_2\text{O}_3$  and (b) nano-CuO.**

In Figure 2(a), the major peaks located at  $2\theta$  values of  $20^\circ$  to  $75^\circ$  correspond to the characteristic diffractions of monoclinic phase CuO [9]. Figure 2(b) can be readily indexed as the rhombohedral crystalline phase [11]. Differential scanning calorimetry (DSC) curves for the thermal decomposition of AP in the presence of nano-sized CuO are illustrated in Figure 3. As can be seen in this figure, the thermal decomposition of pure AP occurs in two stages: the endothermic stage and the exothermic stage. By comparing these four curves, the endothermic stage happens at a temperature of about  $240^\circ\text{C}$ . This stage is related to crystal phase transition from orthorhombic to cubic. The other two peaks at  $314^\circ\text{C}$  and  $455^\circ\text{C}$  are the exothermic peaks that are associated with partial decomposition of AP and the formation of some  $\text{NH}_3$  and  $\text{HClO}_4$  via dissociation and sublimation and complete decomposition of AP and the formation of volatile products, respectively. It is obvious that the addition of nano-sized CuO to AP has no deep effect on the crystallographic phase transition temperature of AP, but it has considerable influence on the exothermic decomposition of AP. Two exothermic peaks are converted to a strong peak in the result of added nano-sized CuO, and this indicates the catalytic activity of nano-sized CuO in the thermal decomposition of AP. During the exothermic process, higher thermal decomposition temperatures of AP with nano-

CuO contents of 1%, 2%, and 3% are 359°C, 348.9°C, and 347.12°C, respectively. At curves b, c, and d of Figure 3, it can be observed that the peaks become steep in the presence of nano-CuO which indicates that the rate of thermal decomposition of AP also increased.

**Figure 3 DSC curves related to (a) pure AP, (b) AP1C, (c) AP2C, and (d) AP3C.**

Figure 4 presents the DSC curves for thermal decomposition of AP in the presence of nano-sized Fe<sub>2</sub>O<sub>3</sub>. From these curves, it can be found out that the thermal decomposition of AP is catalytically affected by nano-sized Fe<sub>2</sub>O<sub>3</sub>. The endothermic stage occurring at a temperature of about 240°C is not greatly influenced by nano-ferric oxide. It is clear that the addition of nano-sized Fe<sub>2</sub>O<sub>3</sub> to AP has a significant effect on the exothermic temperatures of AP. During the exothermic process, higher thermal decomposition temperature of AP with nano-Fe<sub>2</sub>O<sub>3</sub> contents of 1%, 2%, and 3% are 403.57°C, 374.18°C, and 347.87°C, respectively. Rate enhancement of thermal decomposition of AP in the presence of nano-Fe<sub>2</sub>O<sub>3</sub> is drawn from steepness modes of the curves b, c, and d.

**Figure 4 DSC curves related to (a) pure AP, (b) AP1F, (c) AP2F, and (d) AP3F.**

The results associated with decrease in higher thermal decomposition of AP in the presence of nano-sized CuO and nano-sized Fe<sub>2</sub>O<sub>3</sub> are given in Table 2. As it is clear from this table, when nanometer-sized CuO and Fe<sub>2</sub>O<sub>3</sub> are added to AP, the higher decomposition of AP is decreased considerably. From this table, it is obvious that the catalytic effect of adding 1% and 2% of nano-sized CuO with an average particle size of 40 nm is greater than that of the nano-sized Fe<sub>2</sub>O<sub>3</sub> with an average particle size of 20 nm.

**Table 2 Decreased values of higher decomposition temperature of AP**

	AP + nano-sized Fe <sub>2</sub> O <sub>3</sub>			AP + nano-sized CuO		
	3%	2%	1%	3%	2%	1%
Decrease in higher decomposition temperature (°C)	107.13	80.82	51.43	107.88	106.1	96

In Table 3, the results of the catalytic effect of as-synthesized nano-CuO and nano-Fe<sub>2</sub>O<sub>3</sub> in some recent studies are given. As can be seen from this table, the catalytic effect of as-synthesized nano-CuO is higher than that of the as-synthesized Fe<sub>2</sub>O<sub>3</sub>. A similar comparison associated with commercial nano-sized CuO and nano-sized Fe<sub>2</sub>O<sub>3</sub> is also concluded from this study.

**Table 3 Catalytic activity results of as-synthesized nano-sized CuO and nano-sized Fe<sub>2</sub>O<sub>3</sub>**

Sample	Average particle size (nm)	Decrease in higher decomposition temperature of AP (°C)	Reference
AP + nano-CuO (chrysalis-like)	-	85	[9]
AP + nano-CuO	16.5	90.47	[14]
AP + nano-Fe <sub>2</sub> O <sub>3</sub>	30	57	[4]
AP + nano-Fe <sub>2</sub> O <sub>3</sub> (sphere-like)	25	81	[11]
AP + nano-Fe <sub>2</sub> O <sub>3</sub> (pod-like)	-	72	[11]

## Conclusions

The results of differential scanning calorimetry illustrate that nanometer-sized copper oxide and ferric oxide have a significant catalytic effect on the thermal decomposition of ammonium perchlorate. The presence of these nano-sized metal oxides reduces significantly the higher decomposition temperature of ammonium perchlorate. With increase of content of nanometer-sized metal oxide, the decrease in higher decomposition temperature of ammonium perchlorate becomes greater. Also, the catalytic effect of nano-sized copper oxide with larger particle size is more sizable than that of the nano-sized ferric oxide.

## Methods

### Materials

Ammonium perchlorate (monomodal 120  $\mu\text{m}$ ) was purchased from Merck (Darmstadt, Germany). Commercial nano-CuO and nano-Fe<sub>2</sub>O<sub>3</sub> were purchased from Pishgaman Company located in Mashhad, Iran. Physical properties of nano-CuO and nano-Fe<sub>2</sub>O<sub>3</sub> such as bulk density, actual density, specific surface area, and average particle size are given in Table 4. The Chemical compositions of these two nano-sized metal oxides are given in Tables 5 and 6.

**Table 4 Physical properties of nano-CuO and nano-Fe<sub>2</sub>O<sub>3</sub>**

Nano-metal oxide	Bulk density (g/cm <sup>3</sup> )	Actual density (g/cm <sup>3</sup> )	Specific surface area (m <sup>2</sup> /g)	Average particle size (nm)
Nano-CuO	0.79	6.40	20	40
Nano-Fe <sub>2</sub> O <sub>3</sub>	1.20	5.24	40 to 60	20

**Table 5 Chemical composition of nano-CuO**

Element	Mn	Pb	Fe	Mg	P	K	Ca	Sr	Zn	Co	Cd	Ba
Amount (ppm)	3.5	90	87	75	300	300	400	2.3	195	6.4	2.5	0.75

**Table 6 Chemical composition of nano-Fe<sub>2</sub>O<sub>3</sub>**

Element	Mn	Na	Al	S	SiO <sub>2</sub>	P	Cr	Ca
Amount (ppm)	0.095	0.0005	0.0002	0.12	0.134	0.016	0.037	0.024

### Methods

#### *X-ray diffraction analysis*

XRD patterns of nano-CuO and nano-Fe<sub>2</sub>O<sub>3</sub> was performed with a Philips (Amsterdam, The Netherlands) PW 1800 powder X-ray diffractometer using CuK $\alpha$  radiation at 40 kV and 30 mA.

#### *Transmission electron microscopy*

TEM images of nanoparticles were prepared on a Philips (Amsterdam, The Netherlands) transmission electron microscope operated at an accelerating voltage of 100 kV.

### **Differential scanning calorimetry**

The thermal decomposition processes of the samples were characterized by DSC using Dupont (Wilmington, DE, USA) 2000 instrument at a heating rate of 10°C/min.

### **Sample preparation**

The CuO nanoparticles were blent with AP in different contents of 1, 2, and 3 wt.% to prepare the samples for thermal decomposition experiments. These samples were labeled as AP1C (AP + 1% nano-CuO), AP2C (AP + 2% nano-CuO), and AP3C (AP + 3% nano-CuO). Also, in a similar way, the Fe<sub>2</sub>O<sub>3</sub> nanoparticles were mixed with AP, and the samples were labeled as AP1F (AP + 1% nano-Fe<sub>2</sub>O<sub>3</sub>), AP2F (AP + 2% nano-Fe<sub>2</sub>O<sub>3</sub>), and AP3F (AP + 3% nano-Fe<sub>2</sub>O<sub>3</sub>). Before the thermal decomposition experiments using DSC technique, the samples were homogenized. Figures 5 and 6 show the samples used in this study.

---

**Figure 5 AP1C (1), AP2C (2), AP3C (3), and pure AP (4).**

---

**Figure 6 AP1F (1), AP2F (2), AP3F (3), and pure AP (4).**

---

### **Competing interests**

The author has no competing interests.

### **Authors' information**

MM is a student in M.Sc. of Chemical Engineering in Iran University of Science and Technology (IUST).

### **References**

1. El-Sherbiny, IM, Salih, E, Reicha, FM: Green synthesis of densely dispersed and stable silver nanoparticles using myrrh extract and evaluation of their antibacterial activity. *Journal of Nanostructure in Chemistry* **3**, 8 (2013)
2. Maddah, H, Rezazadeh, M, Maghsoudi, M, NasiriKokhan, S: The effect of silver and aluminum oxide nanoparticles on thermophysical properties of nanofluids. *Journal of Nanostructure in, Chemistry* (2013)
3. Hongzhen, D, Xiangyang, L, Guanpeng, L, Lei, X: Synthesis of Co nanoparticles and their catalytic effect on the decomposition of ammonium perchlorate. *Chin J Chem Eng* **16**, 325–328 (2008)
4. Satyawati, SJ, Prajakta, RP, Krishnamurthy, NV: Thermal decomposition of ammonium perchlorate in the presence of nano-sized ferric oxide. *Defense Science Journal* **58**, 721–727 (2008)

5. Duan, H, Lin, X, Liu, G, Xu, L, Li, F: Synthesis of Ni nanoparticles and their catalytic effect on the decomposition of ammonium perchlorate. *Materials Processing Technology* **208**, 494–498 (2008)
6. Farhadi, S, Pourzare, K, Sadeghinejad, S: Simple preparation of ferromagnetic  $\text{Co}_3\text{O}_4$  nanoparticles by thermal dissociation of the  $[\text{Co}^{\text{II}}(\text{NH}_3)_6](\text{NO}_3)_2$  complex at low temperature. *Journal of Nanostructure in Chemistry* **3**, 16 (2013)
7. Weifan, C, Fengsheng, L, Leili, L, Yongxiu, L: Synthesis of nano-sized yttria via a sol–gel process based on hydrated yttrium nitrate and ethylene glycol and its catalytic performance for thermal decomposition of  $\text{NH}_4\text{ClO}_4$ . *Journal of Rare Earths* **24**, 543–548 (2006)
8. Meda, L, Marra, G, Galfetti, L, Severini, F, Luca, LD: Nano-aluminium as energetic material for rocket propellants. *Mater Sci Eng* **C27**, 1393–1396 (2007)
9. Wang, J, He, S, Li, Z, Jing, X, Zhang, M, Jiang, Z: Synthesis of chrysalis-like CuO nanocrystals and their catalytic activity in the thermal decomposition of ammonium perchlorate. *J Chem Sci* **121**, 1077–1081 (2009)
10. Aijun, H, Juanjuan, L, Mingquan, Y, Yan, L, Xinhua, P: Preparation of nano- $\text{MnFe}_2\text{O}_4$  and its catalytic performance of thermal decomposition of ammonium perchlorate. *Chin J Chem Eng* **19**, 1047–1051 (2011)
11. Zhang, Y, Liu, X, Nie, J, Yu, L, Zhong, Y, Huang, C: Improve the catalytic activity of  $\alpha\text{-Fe}_2\text{O}_3$  particles in decomposition of ammonium perchlorate by coating amorphous carbon on their surface. *Journal of Solid State Chemistry* **184**, 387–390 (2011)
12. Zhou, Z, Tian, S, Zeng, D, Tang, G, Xie, C: MOX (M = Zn, Co, Fe)/AP shell-core nanocomposites for self-catalytic decomposition of ammonium perchlorate. *Alloys and Compounds* **513**, 213–219 (2012)
13. Chaturvedi, S, Dave, PN: A review on the use of nanometals as catalysts for the thermal decomposition of ammonium perchlorate. *Journal of Saudi Chemical Society* **17**, 135–149 (2013)
14. Alizadeh-Gheshlaghi, E, Shaabani, B, Khodayari, A, Azizian-Kalandaragh, Y, Rahimi, R: Investigation of the catalytic activity of nano-sized CuO,  $\text{Co}_3\text{O}_4$  and  $\text{CuCo}_2\text{O}_4$  powders on thermal decomposition of ammonium perchlorate. *Powder Technol* **217**, 330–339 (2012)
15. Liu, T, Wang, L, Yang, P, Hu, B: Preparation of nanometer  $\text{CuFe}_2\text{O}_4$  by auto-combustion and its catalytic activity on the thermal decomposition of ammonium perchlorate. *Mater Lett* **62**, 4056–4058 (2008)
16. Duan, G, Yang, X, Chen, J, Huang, G, Lu, L, Wang, X: The catalytic effect of nano-sized MgO On the decomposition of ammonium perchlorate. *Powder Technol* **172**, 27–29 (2007)

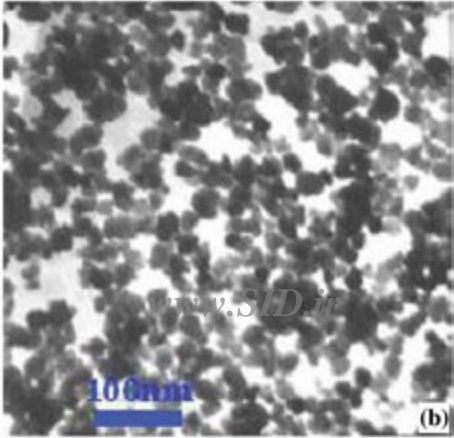
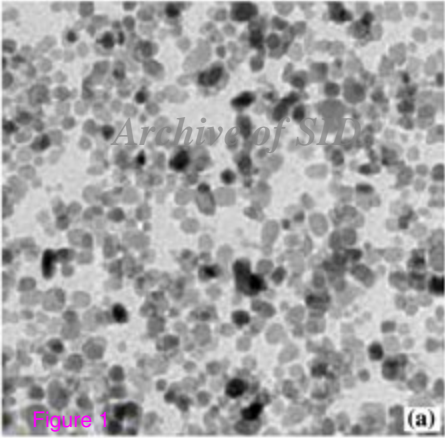


Figure 1

Relative intensity (Counts)

*Archive of SID*

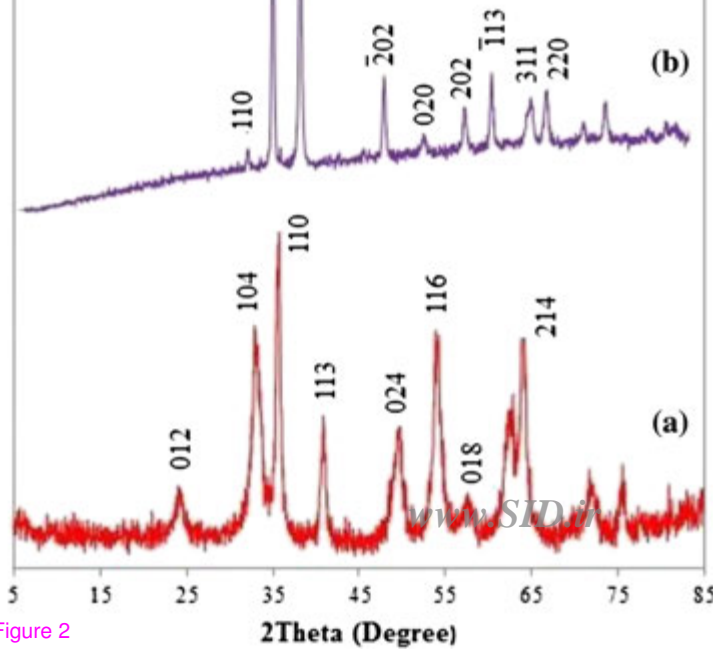
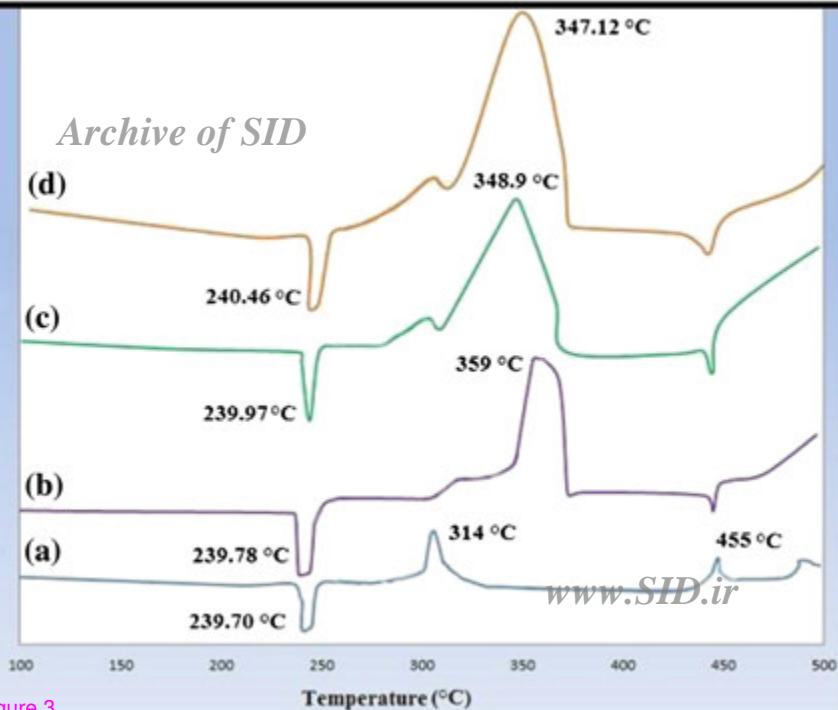


Figure 2



*Archive of SID*

Relative Heat Flow (w/g)



*www.SID.ir*

Figure 3

*Archive of SID*

Relative Heat Flow (w/g)

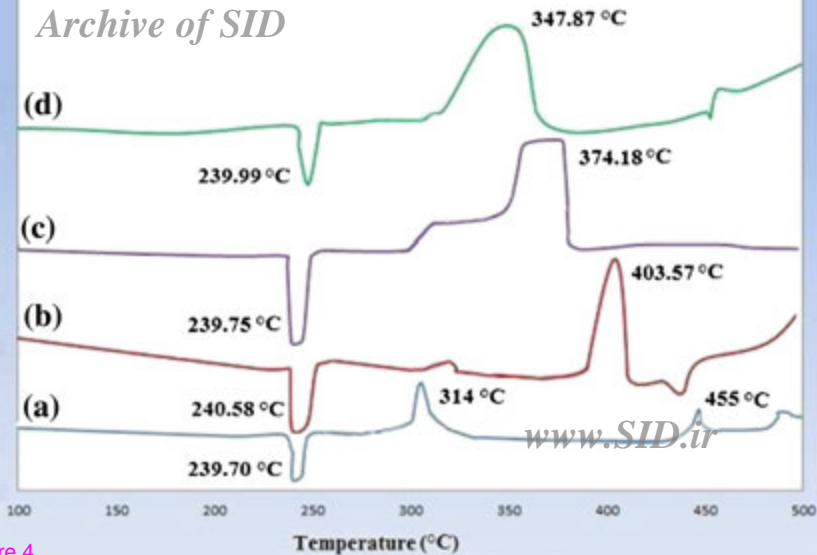


Figure 4

*Archive of SID*

*www.SID.ir*

**(1)**

**(2)**

**(3)**

**(4)**

Figure 5



*Archive of SID*

*www.SID.ir*

**(1)**

**(2)**

**(3)**

**(4)**

Figure 6

